Auditory evoked neuromagnetic response in cerebrovascular diseases: a preliminary study

Kazunori Toyoda, Setsuro Ibayashi, Tomoya Yamamoto, Yasuo Kuwabara, Masatoshi Fujishima

Abstract

***Objectives*—Magnetoencephalography (MEG) measures aspects of the function of the auditory cortex of the human brain with high spatial resolution. The objective was to determine whether MEG also accurately identifies the auditory cortex of the brain in patients with ischaemic stroke.**

***Methods*—The auditory evoked magnetic field (AEF) was examined after stimuli of 1 kHz tone bursts in 24 stroke patients without apparent infarcts in the auditory cortex, and compared the topography of sources of 50 ms (P50m) and 100 ms latency deflections (N100m), the most prominent components of middle and long latency AEFs, with that of 12 normal subjects. Cerebral haemodynamics in and around the auditory cortex were evaluated using PET.**

***Results*—In nine of 24 stroke patients, the accurate magnetic sources of P50m or N100m were not identified. The distribution of P50m sources varied more widely than N100m. Eight of these nine patients had severe stenotic lesions in the carotid or middle cerebral arterial trunks. Patients with abnormal P50m responses had decreased supratemporal and hemispheric blood flow compared with patients with normal P50m responses.**

***Conclusions*—These findings suggest that large vessel disease with disturbed cerebral haemodynamics in and near the auditory cortex tend to affect AEFs, especially the middle latency components. This is the first combined study of MEG and PET to show a significant correlation between AEF responses in stroke patients and their PET indices.**

(*J Neurol Neurosurg Psychiatry* 1998;**64**:777–784)

Keywords: magnetoencephalography; positron emission tomography; functional mapping; ischaemic stroke

Second Department of Internal Medicine
K Toyoda
S Ibayashi
M Fujishima

Department of Otolaryngology
T Yamamoto

Department of Radiology, Faculty of Medicine, Kyushu University, Maidashi 3-1-1, Higashi-ku, Fukuoka 812-82, Japan
Y Kuwabara

Correspondence to:
Dr Kazunori Toyoda, Second Department of Internal Medicine, Faculty of Medicine, Kyusho University, Maidashi 3-1-1, Higashi-ku, Fukuoka 812-8582, Japan. Telephone +81-92-642-5256; fax +81-92-642-5271.

Received 28 July 1997 and in revised form 11 November 1997
Accepted 19 November 1997

Auditory stimuli elicit several magnetic responses—auditory evoked magnetic fields (AEFs)—in the human brain.[1] In the same way as auditory evoked electric potentials (AEPs), AEFs consist of multiple components with early, middle, and long latency. The first represents brain stem responses, and the other two indicate responses in the higher auditory system.[2 3] The most prominent deflections in the middle and long latency AEFs peak at about 40 to 50 ms (P50m) and 100 ms (N100m) after sound onset, respectively.[3–5]

Magnetoencephalography (MEG) permits the mapping of the auditory cortex accurately and non-invasively based on AEFs, although this technique is primarily sensitive to tangential, and not to radial sources. The assumed spatial accuracy of MEG with respect to landmarks on the head was reported to be within 3 mm.[6] Both P50m and N100m are generated in the auditory cortex in the supratemporal plane by combining data derived via MEG and MRI.[6–9] By contrast, the normal profiles of AEFs as disclosed by MEG have not been recorded in some patients with auditory cortical lesions; the auditory response patterns were reported to be totally absent, fairly small, or extremely large in patients with large temporal lobe infarcts.[10 11] On the other hand, patients with infarcts near the supratemporal cortex were shown to have normal responses.[11]

In large vessel cerebrovascular disease, cerebral haemodynamics are often disturbed in broad territories and various hemispheric syndromes are found, even if the infarct documented on MRI is minimal. Occlusive lesions of the carotid and middle cerebral arterial trunks alter auditory cortical circulation and may affect AEFs. The first goal of this study was to examine the hypothesis that MEG may disclose abnormality of the auditory cortex which was not observable in MRI based on AEF responses in stroke patients with large vessel disease.

Positron emission tomography (PET) is a three dimensional imaging technique of brain function. Some PET indices, including regional cerebral blood flow (CBF) and cerebral metabolic rate of oxygen ($CMRO_2$), reflect focal brain activity. These indices have been reported to correlate with electrophysiological findings such as visual evoked potentials and quantitative EEG.[12 13] The second goal of this study was to determine whether abnormalities of PET indices in the auditory cortex correlate with abnormal AEF responses.

Subjects and methods

SUBJECTS

Twenty four right handed patients with chronic non-embolic minor brain infarction (19 men and five women, age range 34 to 75 years) participated in this study. Patients with hearing difficulty and patients without sufficient intellect or endurance for the MEG and PET studies were excluded. Infarcts and causal vascular diseases were evaluated using brain MRI and magnetic resonance angiography (MRA, Sigma System, 1.5 T, GE Co) for all patients. Cervical and transcranial neurosonography

Table 1 Clinical characteristics of the patients

Patient no	*Age (y)/ sex*	*Stroke subtype*	*Affected side*	*Site of infarct in the affected hemisphere*	*Infarct size (cm^2)*	*Vascular pathology of large arteries in the affected side*	*Main symptom*
1	55/M	Large	L	BG	1.8	M1 occlusion	Hemiparesis
2	51/M	Large	L	Putamen	5.2	M1 occlusion	Hemiparesis
3	75/F	Large	L	Frontal Cx–SCx	2.1	M1 stenosis (70%)	Hemiparesis, dysarthria
4	57/M	Large	R	Frontal SCx	0.3	M1 stenosis (90%)	Hemiparesis
5	52/M	Large	L	BG, CR	1.0	M1 stenosis (80%)	Transient hemiparesis
6	69/M	Large	R	SCx	0.4	M1 stenosis (90%)	Transient hemiparesis
7	69/M	Large	R	SCx	0.4	M1 stenosis (80%)	Transient hemiparesis
8	65/M	Large	R	SCx	0.3	ICA occlusion	Asymptomatic
9	65/M	Large	R	BG	2.2	ICA stenosis (>90%)	Hemiparesis
10	68/M	Large	L	BG, SCx	1.0	ICA stenosis (80%)	Syncope
11	71/M	Large	L	BG, CR	1.5	ICA stenosis (80%)	Amnesia
12	73/M	Large	R	Parietal Cx–SCx	6.6	ICA stenosis (70%)	Asymptomatic
13	49/F	Large	R	Parietal Cx–SCx	5.2	ICA occlusion	Amaurosis fugax
14	35/M	Large	R	CR, SCx	5.9	ICA stenosis (90%)	Hemiparesis
15	23/M	Large	L	SCx	0.3	ICA occlusion	Asymptomatic
16	34/M	Large	L	Scx, occipital Cx–SCx	12.5	ICA and PCA occlusion	Hemiplegic migraine
17	67/M	Small	L	SCx	0.3	No significant stenosis	Hemiparesis
18	60/M	Small	L	SCx	0.5	No significant stenosis	Amnesia
19	58/F	Small	L	CR	0.5	No significant stenosis	Asymptomatic
20	53/F	Small	L	SCx	0.3	No significant stenosis	Asymptomatic
21	52/F	Small	L	Thalamus	0.3	No significant stenosis	Hemisensory loss, hemiparesis
22	58/M	Small	R	BG	0.5	No significant stenosis	Amnesia
23	71/M	Small	L	BG, CR, SCx	1.0	No significant stenosis	Gait disturbance
24	57/M	Small	L	Thalamus, BG, CR, SCx	1.9	No significant stenosis	Amnesia

Large=large vessel disease (atherothrombotic infarction, antiphospholipid syndrome, moyamoya-like vasculopathy); Small=small vessel disease (lacunar infarction, Binswanger's disease); L=left; R=right; BG=basal ganglia; Cx=cortex; Scx=subcortex; CR=corona radiata; M1=horizontal trunk of the middle cerebral artery; ICA=internal carotid artery; PCA=posterior cerebral artery.

and conventional cerebral angiography were added to provide further information of vascular lesions.

Twelve right handed normal subjects for the MEG study (MEG control group; six men and six women, age range 21 to 57 years) and another 14 age matched normal subjects for the PET study (PET control group; six men and eight women, age range 39 to 73 years) without hearing difficulty and brain disorders also participated. MRI showed no brain lesions in these control subjects. Informed consent was obtained from all patients and control subjects before MEG and PET studies.

MEG STUDY

MEG was performed in all patients and MEG control subjects using a 37 channel neuromagnetometer (Magnes, Biomagnetic Technologies) in a magnetically shielded room. Each subject lay in the lateral position, and the positions of both preauricular points and the nasion as well as the head shape were measured for each subject using a three dimentional digitiser, and a

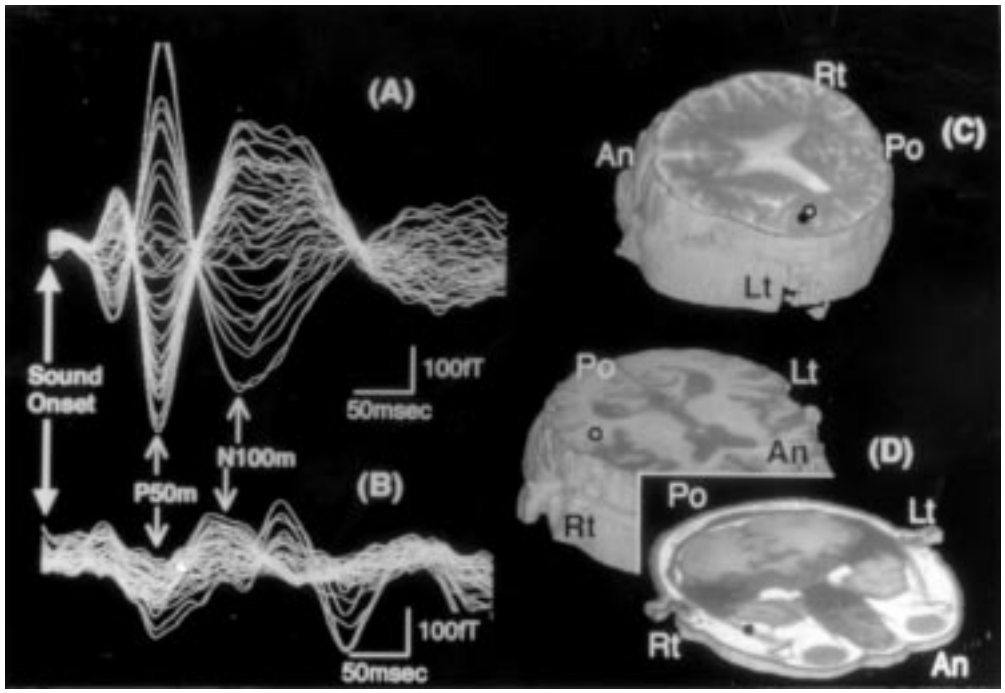

Figure 1 (A, B): Auditory evoked magnetic responses over the left hemisphere of a 57 year old woman from the control group (A) and the responses over the right hemisphere of a 57 year old man with a right frontal subcortical infarction (patient 4, B), recorded by 37 channel MEG. (C, D): Reconstructed three dimensional MRI with magnetic sources for P50m (closed circles) and N100m (open circles) in the 57 year old control subject (C) and Patient 4 (D). An = anterior; Po = posterior; Rt = right; Lt = left.

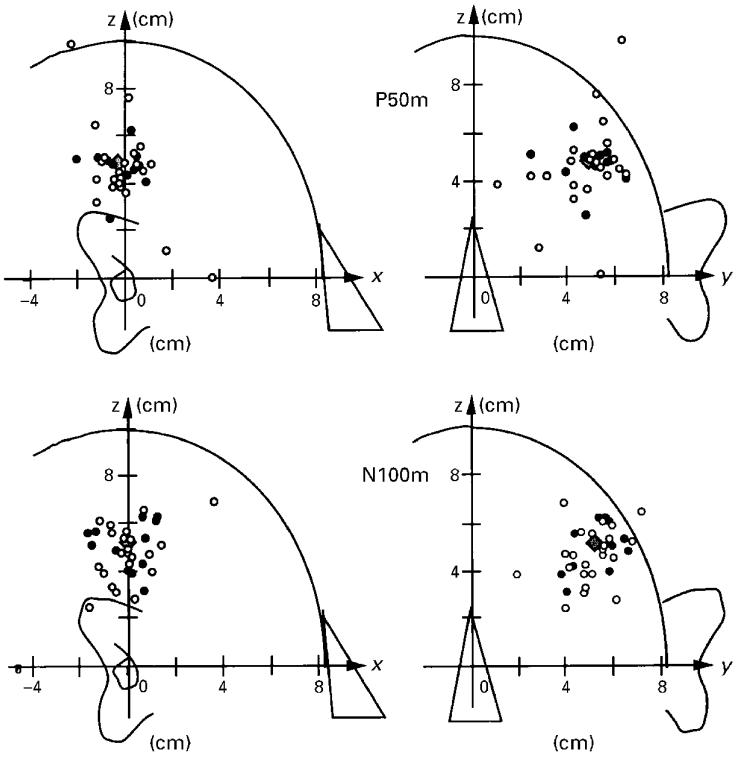

Figure 2 Distribution of the magnetic sources (equivalent current dipoles) of P50m (upper coordinate systems) and N100m (lower coordinate systems) in patients (open circles) and control subjects (closed circles). Rectangles indicate mean source locations for control subjects.

sensor position indicator system. Subjects were instructed to keep their eyes open, to minimise eye movements and eye blinks, and to count silently the number of stimuli. We monitored subjects using a videocamera. Tone bursts of 1 kHz and 50 dB sound pressure level at the ear with 400 ms duration were presented to the patient's ear contralateral to the brain lesion, or the right ear of control subjects, through a 7 m long plastic tube of 15 mm inner diameter terminating in an inserted earphone. Interstimulus intervals varied randomly between 1.5 and 2.5 s around a mean of 2.0 s.

Evoked neuromagnetic fields over the hemisphere contralateral to the stimuli were recorded through a 144 mm diameter circular Dewer positioned close to the temporal region. The detector array was centred on a point 1.5 cm superior to the position T3 of the international 10–20 system, as near as possible to the subject's head. We measured 128 single responses and averaged them with a bandpass of 1 to 55 Hz and a sampling rate of 520 Hz. The auditory components of P50m and N100m were identified by polarity reversals in the subsets of the 37 channels. Peaks of P50m and N100m were visually identified as the points of maximum amplitude, and within a latency window of 25-60 ms and 60-220 ms, respectively, after stimulation. The neuronal current sources corresponding to the peak points of these components were modelled by single equivalent current dipoles (ECDs). The location of ECDs was calculated, and ECDs were superimposed on to the MRI using our previously reported technique.[14 15] ECDs with a correlation coefficient<0.95 between the measured and theoretical fields were discarded from the analysis.

A three dimensional coordinate system was defined for each subject based on both preauricular points and the nasion. The origin is the midpoint between both preauricular points. The x axis joins the origin to the nasion, the y axis passes between the preauricular points, and the z axis is perpendicular to the x-y

Table 2 Magnetoencephalographic and positron emission tomographic findings of the patients

	P50m		*N100m*		*Supratemporal region*			*Entire hemispheric region*		
Patient	*ECD Distance (cm)*	*Correlation coefficient*	*ECD Distance (cm)*	*Correlation coefficient*	*CBF (ml/100 ml/min)*	*OEF*	*$CMRO_2$ (ml/100 ml/min)*	*CBF (ml/100 ml/min)*	*OEF*	*$CMRO_2$ (ml/100 ml/min)*
1	Discarded	0.88	3.6	0.98	27.1	0.435	1.92	22.2	0.456	1.64
2	Discarded	0.92	0.9	0.99	30.7	0.438	2.54	22.4	0.46	1.98
3	8.8	0.96	4.3	0.97	27.5	0.475	2.17	27.5	0.421	1.93
4	6.0	0.95	0.9	0.96	26.8	0.570	2.62	21.3	0.514	1.86
5	2.9	0.98	2.6	0.95	33.7	0.387	2.46	31.7	0.373	2.19
6	1.1	0.96	0.8	0.99	33.5	0.540	2.54	27.7	0.496	1.94
7	1.6	0.99	1.3	0.99	39.7	0.441	2.56	32.5	0.441	2.09
8	1.1	0.99	1.5	0.99	36.0	0.573	2.37	32.5	0.499	1.85
9	0.8	0.99	1.5	0.99	29.4	0.508	3.27	24.4	0.485	2.58
10	1.1	0.99	1.6	0.99	27.4	0.394	2.01	25.5	0.397	1.83
11	1.3	0.99	0.5	0.99	29.3	0.444	2.12	25.3	0.424	1.73
12	1.3	0.99	2.4	0.98	37.4	0.384	2.40	34.0	0.353	2.00
13	1.6	0.99	0.4	0.99	36.4	0.433	2.15	33.3	0.430	1.90
14	4.6	0.95	Discarded	0.80	25.4	0.531	1.83	25.0	0.48	1.66
15	1.4	0.99	3.3	0.99	38.7	0.379	3.08	34.6	0.340	2.44
16	1.9	0.99	1.9	0.99	34.6	0.408	2.10	27.8	0.407	1.68
17	1.4	0.99	1.3	0.99	23.1	0.458	1.55	24.4	0.510	1.47
18	2.5	0.98	2.1	0.98	35.0	0.387	1.55	31.0	0.414	1.47
19	0.3	0.98	1.3	0.98	53.8	0.320	2.89	47.0	0.332	2.60
20	1.9	0.99	1.9	0.99	45.5	0.440	3.57	31.0	0.436	2.39
21	2.1	0.99	1.6	0.99	43.0	0.366	2.41	35.3	0.368	1.99
22	0.8	0.99	0.7	0.98	41.0	0.431	3.38	34.7	0.430	2.82
23	4.0	0.97	1.6	0.99	21.0	0.524	1.98	16.8	0.504	1.49
24	1.1	0.97	0.9	0.99	21.6	0.535	2.24	19.6	0.471	1.80
Patients	2.2 (2.0)	0.97 (0.03)	1.7 (1.0)	0.99 (0.01)	33.2 (8.0)	0.450 (0.069)	2.40 (0.53)	28.6 (6.5)	0.435 (0.055)	1.97 (0.37)
Controls	1.5 (0.7)	0.98 (0.01)	1.6 (0.3)	0.99 (0.004)	41.5 (6.9)	0.396 (0.047)	2.80 (0.38)	34.8 (5.7)	0.406 (0.039)	2.38 (0.20)
p Value	NS	NS	NS	NS	0.0002	0.002	0.003	0.0007	0.03	<0.0001

Underlined data on ECD distance indicate abnormal responses. Controls were 12 normal subjects for MEG or 14 normal subjects (28 regions) for PET. Values of patients and controls are means (SD). CBF=cerebral blood flow; OEF=oxygen extraction fraction; $CMRO_2$=cerebral metabolic rate of oxygen; NS=not significant.

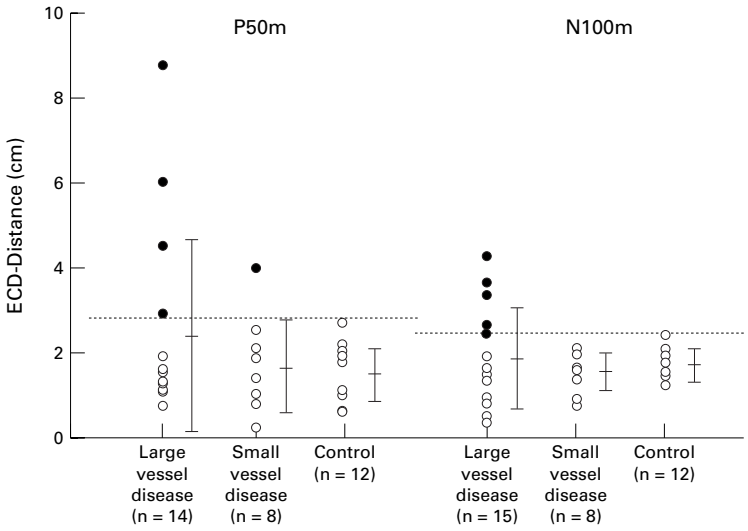

Figure 3 Distances between the equivalent current dipole (ECD) in each patient with large vessel disease, patient with small vessel disease, or control subject and averaged ECD in control subjects (described as ECD-Distance) for P50m and N100m. Bars indicate SD around the mean. Dotted lines indicate mean+2SD of control subjects. Closed circles indicate patients with abnormal ECD localisation whose ECD distance exceed mean+2SD of control subjects.

plane. We regarded the average coordinates of the head size of 12 MEG control subjects as the standard, and corrected the coordinates of ECDs in each patient (or control subject) using the following equation:

$$x = x_0 \times x_N / x_n,\ y = (y_0 \times y_p / y_p) \times (-1)^{\star},$$
$$z = z_0 \times (xN^2 + yP^2 / xn^2 + yp^2)$$

Where (x_0, y_0, z_0)=coordinates of ECD in each patient before correction; x_n=x coordinate of the nasion of each patient; x_N=average of x coordinates of the nasion of control subjects; y_p=y coordinate of the left preauricular point of each patient; y_P=average of y coordinates of the left preauricular point of control subjects; $\star$ only for patients with right side lesions.

PET STUDY

PET was performed in all patients and PET control subjects using a HEADTOME-III device (Shimadzu Inc) with a spatial resolution of 8.2 mm. Each subject lay in the supine position with eyes open and without ear plugs in a semidark room. A small cannula was placed in the femoral artery for arterial blood sampling. Patients underwent this study two days before MEG measurements. Regional CBF, oxygen extraction fraction (OEF), and $CMRO_2$ were measured by the ^{15}O steady state technique, and both OEF and $CMRO_2$ were corrected with cerebral blood volume measured by a single inhalation of $C^{15}O$ gas, as previously described.[16 17] An 18×14 mm rectangular region of interest in the supratemporal cortex ipsilateral to the infarct was identified on an axial slice 50 mm above the orbitomeatal line by visual inspection based on individual MRI findings. Data for the ipsilateral hemisphere were also estimated from the average of all pixels in the entire hemisphere on the same slice.

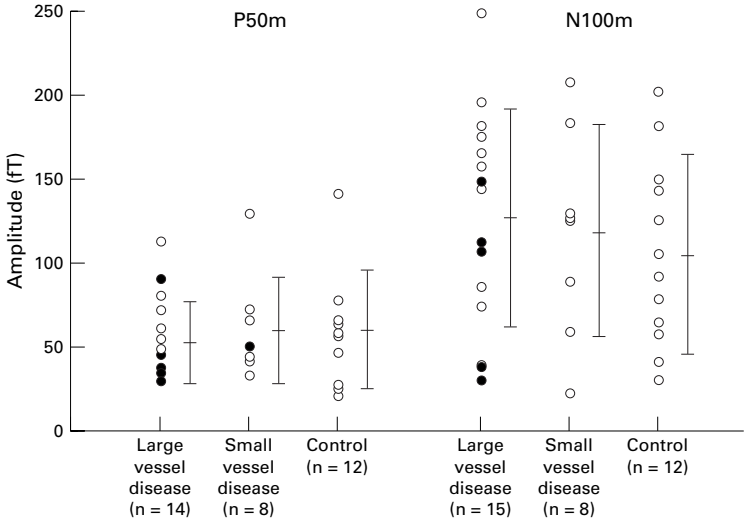

Figure 4 Amplitudes of P50m and N100m in patients with large vessel disease, patients with small vessel disease, and control subjects. Closed circles indicate patients with abnormal localisation of the equivalent current dipole (ECD) (underlined patients in table 2). Bars indicate means (SD).

STATISTICAL ANALYSIS

Values are expressed as means (SD). An unpaired *t* test was used to compare MEG and PET indices. The χ^2 test also was used; $p<0.05$ was accepted as significant.

Results

CLINICAL AND NEURORADIOLOGICAL PROFILES OF PATIENTS (TABLE 1)

Large vessel disease caused infarcts in 16 of 24 patients; 12 (patients 1-12) had atherosclerotic changes, two (patients 13 and 14) had antiphospholipid syndrome derived arterial lesions, and two (patients 15 and 16) had moyamoya-like vasculopathies. Nine of these 16 patients had internal carotid artery lesions (four occlusions and five stenoses) and seven had middle cerebral artery disease (two occlusions and five stenoses). The remaining eight patients did not have severe stenoses in large arteries and were diagnosed as having small vessel disease; six (patients 17–22) were diagnosed as having lacunar infarction, and two (patients 23 and 24) as having Binswanger's disease.

Infarcts in the affected hemisphere lay mainly in the basal ganglia, corona radiata, and cerebral subcortices. Only four patients (patients 3, 12, 13, and 16) had cortical infarcts. Infarcts in the contralateral hemisphere were absent or minimal in all patients. The two patients with small vessel disease (patients 23 and 24) had multiple pontine infarcts, including a cerebellopontine angle infarct in patient 23. In the remaining 22 patients, infarcts in the brain stem either were not detected, or were small and limited to the basis pontis.

MEG FINDINGS

Figure 1 shows typical AEF waveforms from 37 channel MEG recordings of a MEG control subject and one patient (patient 4). Peaks of P50m and N100m were clearly identified in the AEF of the control subject, and their ECDs occurred close together in the supratemporal cortex. By contrast, the waveforms of patient 4 did not have clear P50m and N100m peaks, and the ECD of P50m was remote from the supratemporal cortex. We identified ECDs of

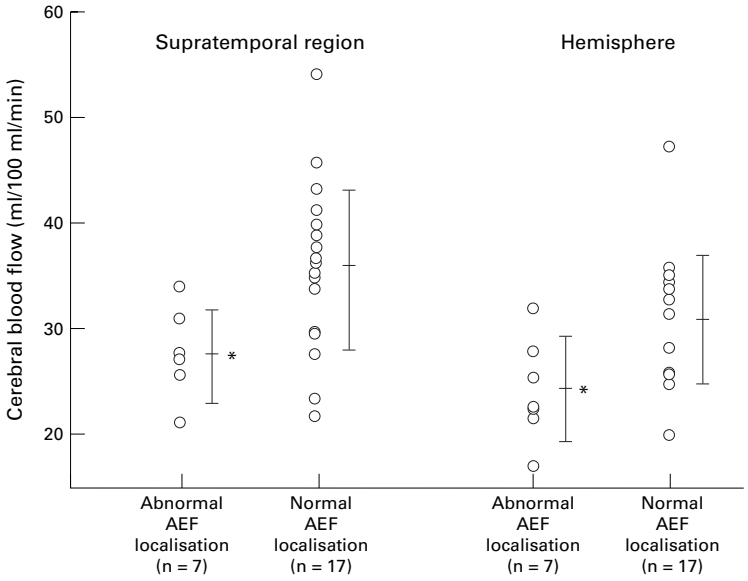

*Figure 5 Regional cerebral blood flow in supratemporal and entire hemispheric regions of patients. Patients with abnormal localisation of the equivalent current dipole (ECD) correspond to underlined patients in table 2. Bars indicate means (SD). *P<0.05 v patients with normal ECD localisation.*

P50m and N100m for all normal subjects, whereas ECDs of P50m in two patients (patients 1 and 2) and that of N100m in one patient (patient 14) were discarded because their correlation coefficients were below 0.95. These three patients had large vessel disease.

x Coordinates of the nasion of control subjects averaged 9.5 (0.9) cm, and y coordinates of their left preauricular point averaged 7.6 (0.8) cm. Figure 2 shows how after correction of coordinates with these data, ECDs of P50m and N100m for patients and control subjects were distributed. x, y, and z Coordinates of ECDs of P50m (cm) averaged (0.2 (1.5), 4.4 (1.7) and 4.6 (2.4) in patients and −0.1 (0.9), 5.0 (1.1) and 4.7 (0.9) in control subjects. Those of N100m averaged 0.1 (1.1), 5.1 (1.1), and 4.6 (1.2) in patients and −0.1 (1.0), 5.3 (1.0), and 5.0 (1.0) in control subjects.

Table 2 and fig 3 show the distances between the ECD of each subject and averaged ECD in control subjects (described as ECD-Distance in the following text, table 2, and figs 3, 6, and 7). ECD-Distances of P50m exceeded the mean+2SD of the control subjects (2.8 cm) in five patients (patients 3, 4, 5, 14, and 23). Four of these five patients had large vessel disease. Correlation coefficients of the P50m ECD in these five patients (0.96 (0.12)) were much lower than those in the remaining 17 patients (0.99 (0.10), p<0.0001). ECD-Distances of the N100m in five patients (patients 1, 3, 5, 12, and 15) exceeded the mean+2SD of the control subjects (2.3 cm). All of these patients had large vessel disease. Correlation coefficients of the ECD in these five patients (0.97 (0.17)) were much lower than those in the remaining 18 patients (0.99 (0.10, p<0.01)). We defined patients with an ECD-Distance over the mean + 2SD of the control subjects or those whose ECD was discarded as the abnormal AEF group in the following analyses. Four patients (patients 1, 3, 5, and 14) had abnormal AEF responses for both P50m and N100m, three (patients 2, 4, and 23) had abnormal AEF responses only for P50m, and two (patients 12, 15) for only N100m (table 2).

Amplitudes of P50m as well as N100m varied widely in both patients and control subjects, and there were no significant differences in these amplitudes between patients (57

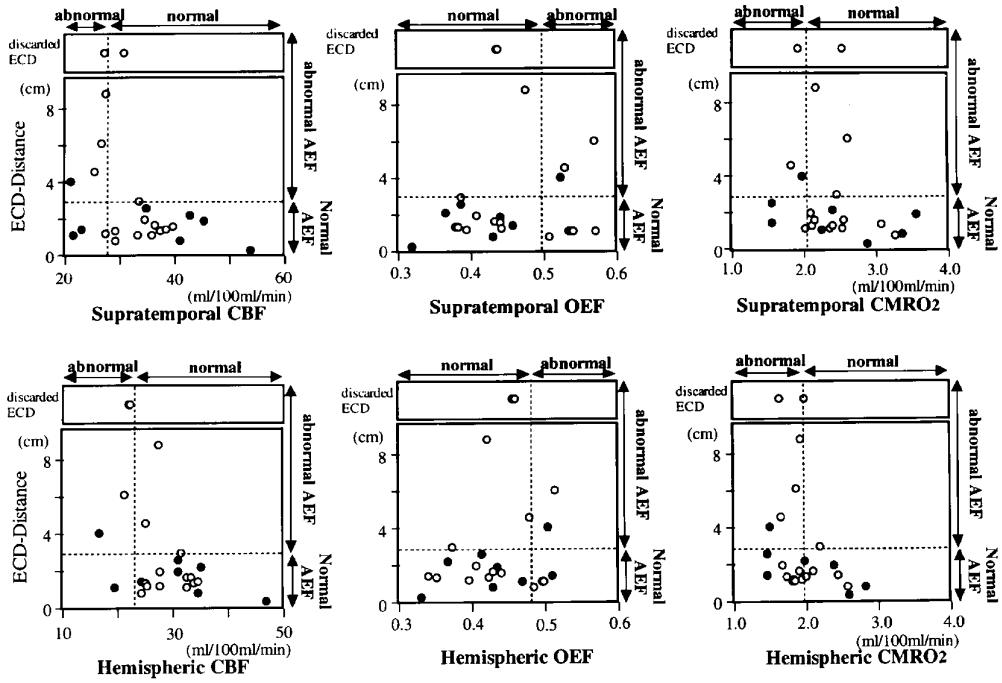

Figure 6 Scattergrams between PET indices in the supratemporal or entire hemispheric regions and the ECD-Distance of P50m in patients with large vessel disease (open circles) and with small vessel disease (closed circles). Equivalent current dipoles (ECDs) with a correlation coefficient of <0.95 between the measured and theoretical fields were discarded.

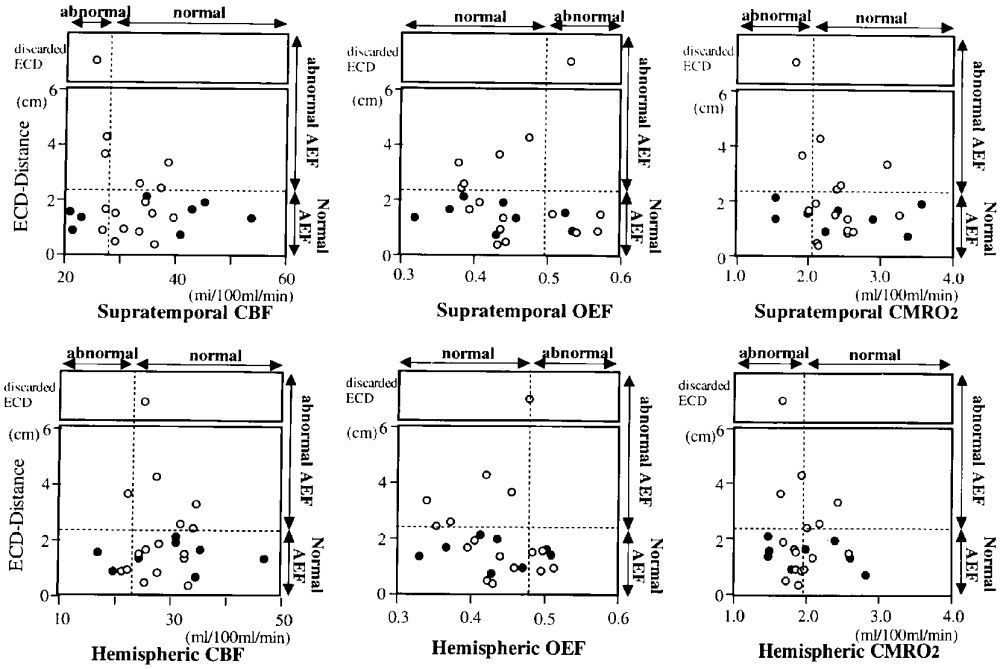

Figure 7 Scattergrams between PET indices in the supratemporal or entire hemispheric regions and the ECD-Distance of N100m in patients with large vessel disease (open circles) and with small vessel disease (closed circles). An equivalent current dipole (ECD) with a correlation coefficient of <0.95 between the measured and theoretical fields was discarded.

(27) fT for P50m and 123 (62) fT for N100m) and control subjects (60 (35) fT for P50m and 105 (58) fT for N100m, fig 4). The above defined abnormal AEF patients had smaller amplitudes of P50m and N100m than patients with normal AEF localisation ($0.05<p<0.1$). There were also no significant differences in latency of P50m and N100m between patients (43 (10) ms for P50m and 94 (15) ms for N100m) and control subjects (43 (10) ms for P50m and 90 (13) ms for N100m).

PET FINDINGS

Regional CBF and $CMRO_2$ were significantly lower, and regional OEF was significantly higher both in the supratemporal and entire hemispheric regions in stroke patients compared with the 14 PET control subjects (table 2). We defined regional CBF and $CMRO_2$ below "mean−2SD" of the control group and regional OEF over mean+2SD of the control group as abnormal data in the following analyses.

Patients with abnormal P50m AEF responses (n=7) had much lower regional CBF (27.5 (4.0) ml/100 ml/min in the supratemporal region and 23.8 (4.8) ml/100 ml/min in the entire hemispheric region) than those with normal AEF responses (n=17, 35.6 (8.1) mll/100 ml/min, and 30.6 (6.2) ml/100 ml/min respectively; $p<0.02$ in both regions, fig 5). Alternatively, there was a significant relation between an abnormal P50m AEF and abnormal regional CBF in the supratemporal region ($p<0.01$) and in the entire hemispheric region ($p<0.005$) by χ^2 test (fig 6). When the same analysis was made using 16 patients with large vessel disease, patients with abnormal P50m AEF responses also had significantly lower regional CBF than those with normal responses ($p<0.01$ in the supratemporal region and $p<0.05$ in the entire hemispheric region). Patients with abnormal responses also had higher regional OEF (0.480 (0.065) in the supratemporal region and 0.458 (0.049) in the entire hemispheric region) and lower regional $CMRO_2$ (2.22 (0.32) ml/100 ml/min in the supratemporal region and 1.82 (0.24) ml/100 ml/min in the entire hemispheric region) compared with those with normal responses (supratemporal OEF, 0.438 (0.068); hemispheric OEF, 0.426 (0.056); supratemporal $CMRO_2$, 2.47 (0.62) ml/100 ml/min; hemispheric $CMRO_2$, 2.04 (0.40) ml/100 ml/min), but this difference was not significant.

Patients with abnormal N100m AEF responses had insignificantly lower regional CBF, OEF, and $CMRO_2$ compared with patients with normal responses (fig 7).

Discussion

There are two major new findings in our study. Firstly, in some patients with large vessel cerebrovascular disease and a small infarct but without any auditory cortical infarcts, the magnetic sources of P50m and N100m were not accurately identified. Distribution of P50m sources varied more widely than those of N100m. Secondly, decreased cerebral perfusion in the auditory cortex and neighbouring territories, as evaluated by PET, correlated with abnormal source localisation of P50m, but not with that of N100m. Thus cerebral perfusion disorders due to large vessel disease tend to affect AEFs, especially the middle latency components.

AUDITORY RESPONSES IN STROKE

Auditory fibres enter the brain stem at the level of the inferior cerebellar peduncle, ascending

through the cochlear nuclei, lateral lemniscus, inferior colliculus, and medial geniculate body, and finally reach the transverse gyri (Heschl) in the supratemporal cortex, the primary auditory area, via the auditory radiations. Any lesions in the pathway may cause auditory dysfunction—for example, supratemporal infarcts affect both magnetic AEF and electric AEP.[10 11 18 19] Lesions of the distal auditory radiations also have been reported to affect AEP.[19]

Our results are unique in that cerebral haemodynamic disorders in and around the supratemporal cortex also cause abnormal AEF responses. The abnormal responses in our patients did not result from heterogeneity of head conductivity or interference of skin potentials, which affect electric evoked potentials but not magnetic fields. Some reports have suggested the possibility of compensatory reorganisation of sensory maps in the human cortex in response to brain injury and infarct.[20 21] However, most of the present abnormal ECDs that were remote from the auditory cortex did not lie in the cerebral cortex, and therefore, cortical reorganisation is not a reasonable explanation for the abnormal localisation of ECDs. In this study, patients with abnormal AEF responses had much lower ECD correlation coefficients and their waveforms did not show symmetric reversals of polarity at the peaks (fig 1). These abnormalities probably caused the abnormal source localisation.

Large vessel disease was a common characteristic of most of the patients with abnormal AEF responses. Localisation of their infarcts varied widely, and all of them were remote from the auditory cortex. Small infarcts in the basal ganglia did not seem to involve the auditory radiations. However, PET detectable territories of decreased perfusion covered both the auditory cortex and auditory radiations in each patient; therefore these flow deficits were thought to be responsible for the abnormal AEF responses.

One patient with an abnormal AEF (patient 23) did not have large vessel disease but a cerebellopontine angle infarct. Disturbance of AEF in this patient may have resulted from direct damage of the primary auditory neurons.

AEF RESPONSES AND CEREBRAL HAEMODYNAMICS

PET permits quantitative evaluation of cerebral circulation and metabolism, and has been widely used as a tool for three dimensional brain functional imaging. Rhythmical electric activities of quantitative EEG seem to correlate well with PET indices.[13] Visual evoked potentials also correlate with regional CBF or local cerebral glucose metabolism in hemianopsic patients.[12] In this study, we expected a similar relation between AEF and PET indices—for example, the presence of a threshold value of regional CBF or $CMRO_2$ below which an abnormal AEF appears.

An abnormal P50m AEF often appeared in patients with a regional CBF below the mean−2SD of CBF in control subjects: 27.7 ml/100 ml/min for supratemporal CBF and 23.4 ml/100 ml/min for the entire hemispheric CBF. These values are equivalent to the ischaemic threshold for reversible neurological deficits in experimental animals.[22] Alternatively, AEF responses were generally normal in patients with supratemporal or entire hemispheric CBF over 30 ml/100 ml/min (fig 4). Significant correlations between AEF and hemispheric CBF suggest that haemodynamic disorders in the territories surrounding the auditory cortex including the medial geniculate body and auditory radiations also affect AEF.

However, $CMRO_2$, another PET index reflecting brain function, did not have a clear correlation with AEF in this study. Some patients with low regional CBF had extremely high OEF for maintenance of normal $CMRO_2$ but still had abnormal AEF responses. The reasons for this phenomenon remain unclear.

Although most of the present patients had small infarcts without obvious brain atrophy, large vessel diseases can cause decreases in brain volume in the affected hemisphere. Thus we cannot exclude the possibility that, besides haemodynamic disorder, changes in brain volume contribute to the difficulties in identifying magnetic sources of P50m or N100m to some extent.

DIFFERENCES IN RESPONSES BETWEEN P50M AND N100M

The previous AEF studies from normal human volunteers usually focused on N100m, which was the largest and most often observed peak in the waveforms.[3–6 8 9] P50m usually has a smaller amplitude as was shown in this study, and accordingly seems to be easily affected by mild brain damage. Thus P50m may be a more sensitive indicator of mild ischaemia in the auditory cortex. This hypothesis is consistent with the present results that abnormal source mapping is more prominent in P50m than in N100m. A greater decrease in regional CBF may be needed to find abnormal source mapping of N100m.

Although the origins of P50m and N100m remain controversial, some reports suggest the possibility of separate origin for these two components.[23] Five patients (patients 2, 4, 12, 15, 23) showed an abnormal AEF response for only one of these two components in the present study, also suggesting the separate generator sources of P50m and N100m. Some reports indicate that abnormalities in middle latency responses are associated with subcortical lesions, or cortical lesions extensive enough to denervate thalamic projection nuclei.[24] In the present study, territories of decreased perfusion detectable by PET in patients with large vessel disease often covered the subcortex surrounding the auditory cortex. Thus subcortical damage may contribute to more severe change of P50m than N100m to some extent.

LIMITATIONS IN THE PRESENT STUDY

We did not routinely measure the AEF in the unaffected hemisphere of stroke patients to shorten time for MEG measurement and lighten the physical burden of patients. One patient with abnormal ECD localisation in his

affected hemisphere had normal ECD localisation in the unaffected hemisphere, and AEF in the unaffected hemisphere was not measured in the remaining eight patients with abnormal AEF response. More precise data of the ECD localisation in the unaffected hemisphere would have brought greater information on the relation between AEF and stroke features.

Stroke patients generally have some disadvantages for MEG measurement, such as alterations in spontaneous cortical activity, decreased cooperation, and motor restlessness during measurement. Although we excluded patients without sufficient intellect or endurance for the present study and all the patients were cooperative, the above disadvantages, especially motor restlessness, might influence the ECD correlation coefficients and identification of P50m and N100m from waveforms to some extent. Aging is another factor which can affect MEG findings. Six of nine patients with abnormal AEF response were under 60 years old, and thus aging does not seem to be a major cause of abnormal localisation of ECD in the present study.

There are some limitations of the control subjects—namely, the fewer subjects and younger age structure than patients. A larger number of controls might represent the healthy population more accurately, and increase the significance of statistical analyses. Although several limitations seem to make our results complicated, we think that the present study can pave the way for further studies on MEG and stroke patients, which have been scarcely reported until now. In a future study, we will involve better age and sex matching of patients and controls.

In conclusion, this is the first combined study of MEG and PET to show a significant correlation between AEF responses in stroke patients and their PET indices. During the era of electric AEPs, neurologists often examined the early components for a topographic diagnosis of brain stem ischaemia or haemorrhage. By contrast, they paid little attention to the middle and long latency components for evaluation of stroke, partly because of technical difficulties in the recording of these components. MEG permits the detection of exact generator areas of these components without major technical problems. This improvement will help clarify the effect of the topography of infarcts or cerebral haemodynamic changes on sensory maps in the human brain.

This work was supported in part by a Research Grant for Cardiovascular Diseases (8A-1, to S I) from the Ministry of Health and Welfare, Japan. We thank Dr Hiroshi Shigeto, Department of Neurology, Kyushu University and Ms Yuko Somehara, Biomedical Division, Sumitomo Metal Ind, Ltd, for their technical assistance with MEG, Dr Masayuki Sasaki, Department of Radiology, Kyushu University, for his technical assistance with PET, and Dr Michael Carrithers for editing the English.

1 Reite M, Edrich J, Zimmerman JT, *et al*. Human magnetic auditory evoked fields. *Electroencephalogr Clin Neurophysiol* 1978;**45**:114–7.
2 Picton TW, Hillyard SA, Krausz HI, Galambos R. Human auditory evoked potentials. I: Evaluation of components. *Electroencephalogr Clin Neurophysiol* 1974;**36**:179–190.
3 Hari R, Aittoniemi K, Järvinen ML, *et al*. Auditory evoked transient and sustained magnetic fields of the human brain. Localization of neural generators. *Exp Brain Res* 1980;**40**: 237–40.
4 Farrel DE, Tripp JH, Norgren R, *et al*. A study of the auditory evoked magnetic field of the human brain. *Electroencephalogr Clin Neurophysiol* 1980;**49**:31–7.
5 Romani GL, Williamson SJ, Kaufman L, *et al*. Characterization of the human auditory cortex by the neuromagnetic method. *Exp Brain Res* 1982;**47**:381–93.
6 Yamamoto T, Williamson SJ, Kaufman L, *et al*. Magnetic localization of neuronal activity in the human brain. *Proc Natl Acad Sci USA* 1988;**85**:8732–6.
7 Reite M, Teale P, Zimmerman J, *et al*. Source location of a 50 msec latency auditory evoked field component. *Electroencephalogr Clin Neurophysiol* 1988;**70**:490–8.
8 Pantev C, Hoke M, Lehnertz K, *et al*. Identification of sources of brain neuronal activity with high spatiotemporal resolution through combination of neuromagnetic source localization (NMSL) and magnetic resonance imaging (MRI). *Electroencephalogr Clin Neurophysiol* 1990;**75**:173–84.
9 Papanicolaou AC, Baumann S, Rogers RL, *et al*. Localization of auditory response sources using magnetoencephalography and magnetic resonance imaging. *Arch Neurol* 1990;**47**:33–7.
10 Leinonen L, Joutsiniemi SL. Auditory evoked potentials and magnetic fields in patients with lesions of the auditory cortex. *Acta Neurol Scand* 1989;**79**:316–25.
11 Mäkelä JP, Hari R, Valanne L, *et al*. Auditory evoked magnetic fields after ischemic brain lesions. *Ann Neurol* 1991;**30**:76–82.
12 Celesia GG, Polcyn RD, Holden JE, *et al*. Visual evoked potentials and positron emission tomographic mapping of regional cerebral blood flow and cerebral metabolism: can the neuronal potential generators be visualized? *Electroencephalogr Clin Neurophysiol* 1982;**54**:243–56.
13 Nagata K, Tagawa K, Hiroi S, *et al*. Electroencephalographic correlates of blood flow and oxygen metabolism provided by positron emission tomography in patients with cerebral infarction. *Electroencephalogr Clin Neurophysiol* 1989;**72**:16–30.
14 Morioka T, Yamamoto T, Katsuta T, *et al*. Presurgical three-dimensional magnetic source imaging of the somatosensory cortex in a patient with a peri-Rolandic lesion: technical note. *Neurosurgery* 1994;**34**:930–4.
15 Minami T, Gondo K, Yamamoto T, *et al*. Magnetoencephalographic analysis of rolandic discharges in benign childhood epilepsy. *Ann Neurol* 1996:**39**;326–34.
16 Fujii K, Sadoshima S, Okada Y, *et al*. Cerebral blood flow and metabolism in normotensive and hypertensive patients with transient neurologic deficits. *Stroke* 1990;**21**:283–90.
17 Yao H, Sadoshima S, Ibayashi S, *et al*. Leukoaraiosis and dementia in hypertensive patients. *Stroke*. 1992;**23**:1673–7.
18 Knight RT, Hillyard SA, Woods DL, *et al*. The effects of frontal and temporal-parietal lesions on the auditory evoked potential in man. *Electroencephalogr Clin Neurophysiol* 1980;**50**:112–24.
19 Scherg M, Von Cramon D. Evoked dipole source potentials of the human auditory cortex. *Electroencephalogr Clin Neurophysiol* 1986;**65**:344–60.
20 Yang TT, Gallen C, Schwartz B, *et al*. Sensory maps in the human brain. *Nature* 1994;**368**:592–3.
21 Lewine JD, Astur RS, Davis LE, *et al*. Cortical organization in adulthood is modified by neonatal infarct: a case study. *Radiology* 1994;**190**:93–6.
22 Jones TH, Morawetz RB, Crowell RM, *et al*. Thresholds of focal cerebral ischemia in awake monkeys. *J Neurosurg* 1982;**54**:773–82.
23 Pelizzone M, Hari R, Mäkelä JP, *et al*. Cortical origin of middle-latency auditory evoked responses in man. *Neurosci Lett* 1987;**82**:303–7.
24 Woods DL, Clayworth CC, Knight RT, *et al*. Generators of middle- and long-latency auditory evoked potentials: implications from studies of patients with bitemporal lesions. *Electroencephalogr Clin Neurophysiol*. 1987;**68**:132–48.